# TUNNELING, RAMAN AND STM STUDIES OF THIN YBaCuO FILMS*

RYSZARD CZAJKA, MAREK KOZIELSKI and BRONISŁAW SUSŁA

Institute of Physics, Poznań Technical University, ul. Piotrowo 3, 60-965 Poznań, Poland

ADAM WITEK, ANDRZEJ REICH and JERZY RAUŁUSZKIEWICZ

Institute of Physics, Polish Academy of Sciences, Al. Lotników 32/46, 02-668 Warszawa, Poland

ABSTRACT. Tunnel junctions with high-$T_c$ superconductor thin film (dc-sputtered from $YBa_2Cu_3O_{7-x}$ target) as tunnel barrier were obtained. Tunnel characteristics with zero-bias anomaly in $dI/dV$ suggest amorphous nature of thin YBaCuO film. The Raman and $d^2V/dI^2$ spectra prove that the layers obtained have semiconducting $YBa_2CuO_5$ structure and are probably doped with $BaCuO_2$. The Scanning Tunneling Microscope (STM) surface topography of YBaCuO layers shows the amorphous nature before annealing and some structure features – the emerging of grain boundaries – after annealing.

## 1. INTRODUCTION

Single crystals and thin films of the layered copper-oxide perovskite-type materials have been under intensive investigation since 1986, when J.G. Bednorz and K.A. Müller [1] started their pioneering work on high-$T_c$ superconductors. Optical spectroscopies [2, 3], electron tunneling [4] and point-contact tunnel spectroscopy [5] as well as the scanning tunneling microscope (STM) [6–8] are often used to study bulk material and thin films of YBaCuO.

In this work we have attempted to obtain planar metal-insulator-metal (MIM) junctions with YBaCuO perovskite thin film as barrier. Raman and inelastic electron tunneling spectra of thin YBaCuO films obtained by the dc-sputtering method were taken to obtain structure information.

The YBaCuO thin film topography was measured by STM connected with the computer data acquisition system at the Institute of Physics of the Polish Academy of Sciences in Warsaw.

A brief review of the literature data is given in chapters 2 (Raman spectra), 3 (Electron tunneling spectra) and 4 (STM investigations). The experimental details, the authors' results and a discussion are presented in chapters 5, 6 and 7.

---

## 2. RAMAN INVESTIGATIONS

There were some difficulties in the way of detailed studies of the lattice vibration of high-$T_c$ superconductors by Raman scattering. One of the reasons for this is the weakness of the Raman signal from high superconducting materials. Morioka et al. [2] have measured Raman spectra of polycrystalline samples of orthorhombic $YBa_2Cu_3O_{7-x}$, its Ho- and Nd-analogs, metastable tetragonal $YBa_2Cu_3O_{7-x}$ and $Y_2BaCuO_5$ (green phase) at room temperature by means of a multichannel spectrometer. They obtained five Raman bands in orthorhombic $YBa_2Cu_3O_{7-x}$ with a strong characteristic Cu–O stretching mode at about 500 $cm^{-1}$ and broad, weak bands around 430–440 $cm^{-1}$, the band at 338 $cm^{-1}$ which is related to the vibration in the vicinity of the Y site, and the 148 $cm^{-1}$ and 115 $cm^{-1}$ bands considered to be related to the structure in the vicinity of the Ba site.
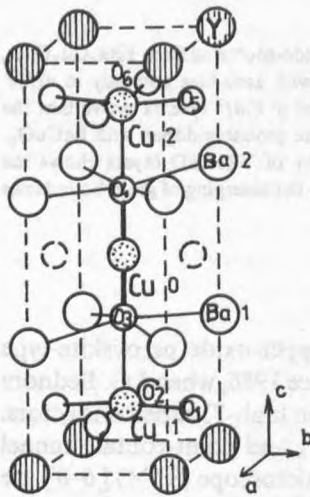


Fig. 1. Atomic positions in the orthorhombic $YBa_2Cu_3O_{7-x}$ unit cell.

A more systematic approach has been made by R. Bhadra et al. [3]. They reported Raman scattering experiments from high-$T_c$ superconductors of the $RBa_2Cu_3O_{7-x}$ type with R = Y, Pr, Nd, Eu, Gd, Dy and Yb. Because of the great difficulty in obtaining single-phase samples, spectra from all starting compounds and other known phases of Y–Ba–CuO were presented. The lines originating in the superconducting yttrium compound were investigated as functions of the quench temperature and oxygen deficiency. Bhadra et al. have identified Raman lines from $YBa_2Cu_3O_{7-x}$ close to the Morioka values at 116, 149, 336, 434 and 504 $cm^{-1}$. From the dependence of oxygen stoichiometry the 336 $cm^{-1}$ line is assigned to a defect-induced Raman mode and is intense only in samples which have a high oxygen deficiency. The remaining four modes are found to have $A_g$ symmetry and mass considerations suggest that the 116 and 149 $cm^{-1}$ bands arise from vibrations of Cu(2) and Ba atoms. Furthermore, the 434 and 504 $cm^{-1}$ lines are assigned to O(4) and O(2)+O(3) vibrations (the atomic positions as marked in Fig. 1).

M. Hangyo et al. [9] found that the Raman band associated with oxygen vibrations observed at $\simeq 500$ $cm^{-1}$ is very sensitive to the oxygen content. Its frequency shifts continuously from 502 to 484 $cm^{-1}$ and this band can be used to determine the oxygen content in $YBa_2Cu_3O_{7-x}$. The 148 $cm^{-1}$ line shows a similar dependence. The frequencies of the 502 and 148 $cm^{-1}$ bands increase almost linearly with the oxygen content respectively at rates of 26 and 10 $cm^{-1}$ per one oxygen atom in the formula. In contrast to Bhadra's results [3] Hangyo

found that the frequency of the 340 cm$^{-1}$ band is almost independent of the oxygen stoichiometry. The Hangyo results are presented in Fig. 2.

Phonon Raman scattering in orthorhombic and tetragonal $YBa_2Cu_3O_{7-x}$ at different temperatures was measured by Nakashima *et al.* [10]. No remarkable temperature dependence was observed for the phonon modes above 100 cm$^{-1}$ for 33 K and 300 K. This result is consistent with that of McFarlane *et al.* [11]. Each phonon band except 340 cm$^{-1}$ is shifted to the higher frequency side on cooling. The frequency shift from 33 K temperature up to 300 K is only by several wave numbers for each mode, e.g. the 502 cm$^{-1}$ band shifts to 506 cm$^{-1}$ for the orthorhombic phase and from 486 to 490 cm$^{-1}$ for the tetragonal phase of $YBa_2Cu_3O_{7-x}$.
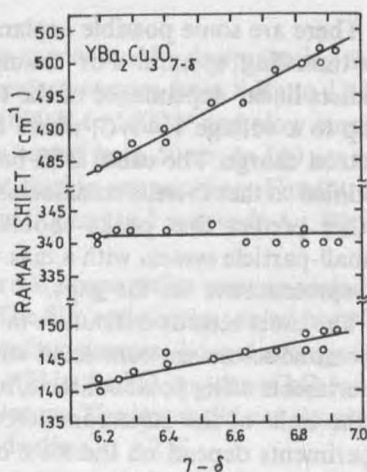
Fig. 2. The frequencies of the three strong bands plotted as functions of the oxygen content $7-\delta$ [9].

## 3. ELECTRON TUNNELING SPECTROSCOPY STUDIES OF HIGH-$T_c$ SUPERCONDUCTORS

Electron Tunneling Spectroscopy (ETS) is a widely recognized and applied diagnostic tool in the field of superconductivity. Since its discovery by Giaever in 1960 [12], ETS has provided the most complete characterization of the superconducting state.

ETS is realized in tunnel junctions. A tunnel junction consists of two conducting electrodes separated by a thin (2–5 nm) insulator (or vacuum). The tunnel current depends on tunneling probability which characterizes the barrier and the electronic densities of states in both electrodes. All ETS information can be deduced from the analysis of $I$–$V$ (or $dI/dV$, $d^2I/dV^2$) *vs.* $V$ ($V$ – the bias voltage) characteristics, e.g. the superconductivity gap. However, in an application of ETS to a new kind of superconductors, it turned out that the results were not convincing, not consistent with each other, not reproducible and difficult to interpretation in terms of well-known pairing mechanisms. In general, the tunneling $dI/dV$ (or $dV/dI$) spectra measured on the high-$T_c$ superconductors exhibit some typical peculiarities: (a) great zero-bias anomalies, (b) many peaks in $dV/dI$ symmetric in bias, (c) the temperature dependence of the positions of these peaks does not follow the $\Delta(T)$ dependence of BCS superconductors [4] ($\Delta$ – superconductor energy gap).

There are some possible explanations of the nature of the multiple peaks in the tunneling spectra. For example, the Zeller-Giaever model [13] which predicts linear dependence of the tunneling conductance $dI/dV$ vs. bias voltage $V$ up to a voltage $V = e/C$, where $C$ is the mean grain capacitance and $e$ is the electron charge. The usual BCS behaviour – zero conductance up to $V = \Delta/e$ is modified so that there is no associated peak in DOS at $V = \Delta/e$. Mullen et al. [14] further predict that peaks should appear in $dI/dV$ tunnel characteristics of a small-particle system with a bias-voltage spacing of $e/C$ and the first peak may be representative for the gaps.

The most serious difficulties in the application of ETS diagnostic to high-$T_c$ superconductors are connected with degradation of the surface. For tunneling experiments using point contacts, tunneling occurs between a tip and a few grains in the bulk of the superconductor. The tunnel gap widths obtained in these experiments depend on the state of the grains.

Generally, a variable gap is found and it is an indication that the sample is not a uniform, well defined superconductor but consists of a mixture of both normal and superconducting regions with variable superconducting properties [4].

### 4. STM STUDIES OF HIGH-$T_c$ SUPERCONDUCTORS

Several research centres use the Scanning Tunneling Microscope (STM) to study the surface of high-$T_c$ superconductors. Most of them have performed measurements in air, scanning the surfaces of broken pellets with a tungsten tip.

Van de Leemput et al. [6] have measured the (001) surface of $YBa_2Cu_3O_7$ single crystals and found evidence that the bulk orthorhombic crystal structure extends to the surface. Growth steps were observed with a height corresponding to the unit of the $c$-axis and there was no evidence for semiconducting behaviour of the surface.

Okoniewski et al. [7] found that slow scanning images show surface roughness in agreement with scanning electron microscope observations. Fast scanning images show the structure with dimensions comparable with those of the bulk layered perovskite unit cell of the material.

Laiho et al. [8] found relatively flat plateaus with dimensions of more than $1~\mu m \times 1~\mu m$, various step formation and special stripe structures with stripe widths about 100 nm and more. On the other hand, they observed prolonged steps and flake-like walls with heights starting from a few unit cell dimensions.

### 5. THIN FILM AND JUNCTION TECHNOLOGY

Corning glass, polycrystalline $BaTiO_3$, $Al_2O_3$ and sapphire were used as substrates. Base metal electrodes were evaporated onto these substrates in the form of 1 mm wide Au, Ni or V strip by thermal evaporation or by electron gun in

$10^{-4}$ Pa vacuum. Afterwards, the thin film was evaporated by dc-sputtering from $YBa_2Cu_3O_{7-x}$ target in argon atmosphere under pressure from 8 Pa to 12 Pa. The high dc-voltage was within the range of 1000 V to 1600 V and glow current from 10 mA to 20 mA. The thin film thickness varied from 50 nm to 600 nm and was dependent on the time and glow current during evaporation. Finally, the outer electrodes were evaporated in the form of 0.2 mm to 1 mm wide Au, Pb, Ni or V crossed strips.

Some of these thin films before outer electrode evaporation were annealed in an oxygen or air atmosphere for 4 to 8 hours. The film resistivities varied from 0.1 $M\Omega$ to 30 $M\Omega$ (along the surface). The annealing process did not change the resistivity of these layers distinctly, and it was still in the $k\Omega$- or tens of $k\Omega$-range and increased to 1 $M\Omega$ with decreasing temperature. The layers did not show the metallic conductivity and were not superconducting at 4.2 K.

## 6. EXPERIMENTAL DETAILS

$I-V$ and its derivatives characteristics were measured by standard 4-terminals and harmonic detection methods [15] at liquid helium temperature.

Raman polarized spectra were measured at room temperature using back-scattering geometry (180° scattering angle). An ILA-120 Carl-Zeiss Jena Laser operating at 488 nm with the output power 100 mW was used as light source. Occasionally the 458 line was also used. The scattered light was analyzed with a GDM-1000 Monochromator and detected with a cooled EMI-9658B photomultiplier. The experimental setup permitted the band positions in the Raman spectra to be estimated with an accuracy of $\pm 4$ cm$^{-1}$.

The STM employed in our experiment is a modified version of the design described by Binnig and Smith [16]. The modification consists in the application of a bimorph membrane as a $z$-piezodrive for the fine distance control. The details of this STM set are given in [17]. The STM images were taken in air, under atmospheric pressure for thin YBaCuO films obtained by dc-sputtering on sapphire substrate with Au as buffer layer.

## 7. RESULTS AND DISCUSSION

Many tunnel junctions were either short-circuited or of $M\Omega$ order resistivity. The evaporated material was simply porous ceramic enabling shorting by metallic microbridges on the one hand or creating a barrier too thick for tunneling on the other. Nevertheless, for tens of junctions we obtained nonlinear $I-V$ curves of the suitable resistivities and their first derivatives exhibited large zero-bias anomaly similar to those reported by Hohn *et al.* [5]. Figure 3 represents typical $I-V$, $dV/dI$ and $d^2V/dI^2$ characteristics for V–YBaCuO–Pb junction measured at 4.2 K.
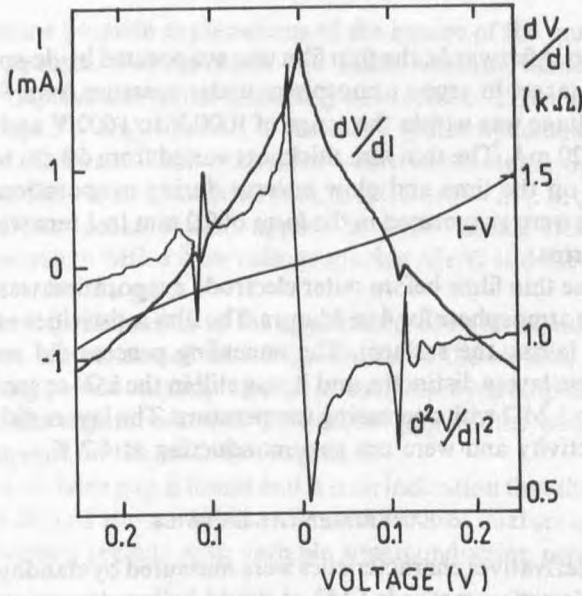
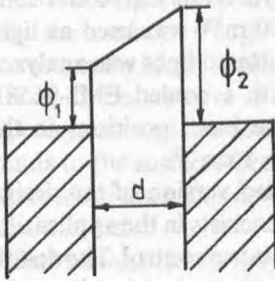Fig. 3. Typical tunnel characteristics of Me–YBaCuO–Me junctions.



Fig. 4. Tunnel barrier model in M–I–M junction.

In spite of the large zero-bias anomaly it was difficult to obtain the oscillating and vibrating excitations spectra inside the YBaCuO barrier. However, using a bridge with harmonic detection [6] and a computer data acquisition system we obtained $d^2V/dI^2$ spectra in the range of zero-bias anomaly (up to 0.1 eV or 800 cm$^{-1}$), where the junction resistivity changes rapidly.

The nonlinear $I - V$ characteristics prove that YBaCuO thin film constitutes the tunnel barrier or a part of the tunnel barrier in MIM junctions. If one assumes a trapezoidal shape of the barrier described by left and right barrier heights $\Phi_1$, $\Phi_2$ and a barrier width $d$ (Fig. 4), then the barrier may be represented by the expression

$$\Phi(z) = \Phi_1 + \frac{z}{d} \cdot (\Phi_2 - \Phi_1) \tag{1}$$

and the tunnel current by

$$j = 1.6185 \cdot 10^{11} \cdot \left\{ V \cdot \int_V^\eta D(u) \cdot du + \int_0^V D(u) u \cdot du \right\} \tag{2}$$

where $j$ is the current density in [mA/mm$^2$], $V$ bias voltage in [V], $u = \eta - E_z$, $\eta$ the Fermi level measured from the conduction band bottom, and $E_z$ the electron

energy in the z-direction (perpendicular to the junction surface). $D(u)$ can be expressed by:

$$D(u) = \exp\left\{-0.6831 \cdot \int_0^d [\Phi(z) + u]^{1/2} \cdot \tfrac{3}{2} \delta z\right\}, \tag{3}$$

where: $d$ is the barrier width in [Å], $u$, $\Phi$ in [eV].

This barrier analysis has been proposed by Korman *et al.* [18]. The computer program was based on the algorithm proposed by Hipps *et al.* [19]. Table I shows the calculated values of the barrier parameters. The barrier parameters suggest that the barrier is probably caused by surface degradation of bulk YBaCuO so that the barrier heights are relatively low but the junction width is large.

TABLE I

Tunnel barrier parameters calculated from $I - V$ characteristics for junctions with YBaCuO as barrier.

| Junction type | $\Phi_1$ [eV] | $\Phi_2$ [eV] | $d$ [nm] |
|---|---|---|---|
| Al–YBaCuO–Al | 0.47 | 0.95 | 2.28 |
|  | 0.62 | 0.42 | 2.52 |
| Au–YBaCuO–Al | 0.18 | 0.28 | 3.33 |
|  | 0.73 | 1.21 | 2.67 |
| V–YBaCuO–Pb | 1.33 | 2.22 | 2.27 |
| V–YBaCuO–V | 0.93 | 0.93 | 2.16 |
| V–YBaCuO–Au | 0.26 | 0.23 | 4.22 |

IETS spectra of MIM junctions with YBaCuO thin film as barrier are presented in Figs. 5a and 5b. They are compared with the Raman spectrum of the same film (Fig. 5c) and with other literature Raman data – Figs. 5d, 5e and 5f [2, 3].

IETS spectra of V–YBaCuO–V and V–YBaCuO–Pb junctions (Fig. 5a and 5b) contain lines of about 210 cm$^{-1}$, 580 cm$^{-1}$, 625 cm$^{-1}$ and a wide band between 300 cm$^{-1}$ and 400 cm$^{-1}$. The Raman spectrum of the same thin film (Fig. 5c) not annealed in oxygen contains lines: 331 cm$^{-1}$, 447 cm$^{-1}$, 595 cm$^{-1}$ and 624 cm$^{-1}$. These lines were compared with the literature data of Raman spectra of $Y_2BaCuO_5$ (Fig. 5d), $BaCuO_2$ (Fig. 5e) and orthorhombic $YBa_2Cu_3O_{7-x}$ (Fig. 5f).

A final conclusion from the above results is that the not annealed YBaCuO thin films obtained by dc-sputtering do not possess the orthorhombic structure characteristic for high-$T_c$ superconductors; especially, there is a lack of the 502 cm$^{-1}$ line, attributed to the vibration of oxygen atoms in $YBa_2Cu_3O_{7-x}$, but they have the semiconducting phase structure of $Y_2BaCuO_5$ and are probably doped with $BaCuO_2$ as an intermediate compound. The presence of $Y_2BaCuO_5$ structure was confirmed by further annealing of the sample in air, when the so-called "green phase" was visible.
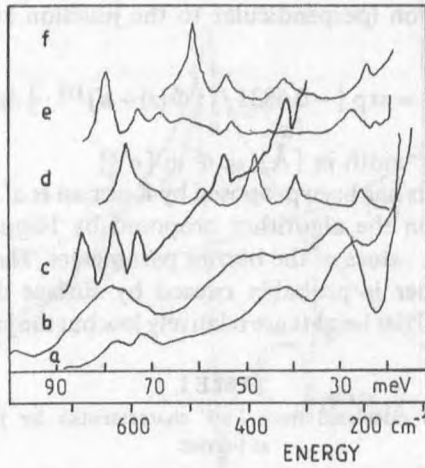
Fig. 5. IETS spectra of V–YBaCuO-V (a), and V–YBaCuO-Pb (b) junctions and Raman spectra of thin YBaCuO film (c), $Y_2BaCuO_5$ (d) [2], $BaCuO_2$ (e) [3], and $YBa_2Cu_3O_{7-x}$ (f) pellets [2].
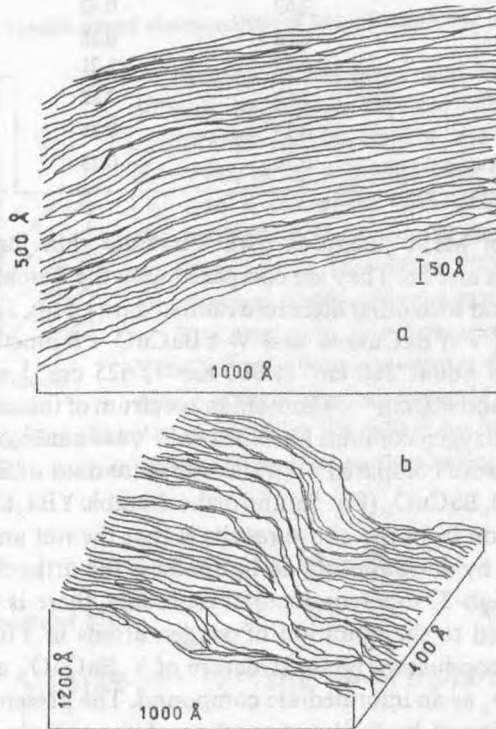


Fig. 6. STM images of YBaCuO layer before (a) and after annealing (b).

The STM images of YBaCuO thin film show that the surfaces seem to be smooth with no distinct structures before annealing in oxygen atmosphere (Fig. 6a). After the annealing process we observe changes in surface structure connected with possible crystallization, and the appearing of grain boundaries (Fig. 6b) resembling the flake-like walls described by van de Leemput [6].

More detailed STM studies of $YBa_2Cu_3O_{7-x}$ thin film samples will be carried out in the nearest future.

## ACKNOWLEDGEMENTS

## REFERENCES

[1] J.G. Bednorz and K.A. Müller, *Z. Phys. B - Condensed Matter* **64**, 189 (1986).

[2] Y. Morioka, M. Kikuchi and Y. Syono, *Jap. J. of Appl. Phys.* **26** L1499 (1987).

[3] R. Bhadra, T.O. Brun et al., *Phys. Rev.* **B37**, 5142 (1988).

[4] J. Raułuszkiewicz, "Energy Gap in High-$T_c$ Superconductors Studied by Means of Electron Tunneling Spectroscopy" – to be published in: Proceedings of the 4-th International Conference on the Physics of Magnetic Materials, Szczyrk-Biła, Poland, September 4–10, 1988: World Scientific, Singapore.

[5] N. Hohn, R. Koltun, H. Schmidt, S. Blumenröder, H. General et al., *Z. Phys. B - Condensed Matter* **69**, 173 (1987).

[6] L.E.C. van de Leemput, P.J.M. van Bentum, L.W.M. Schreurs and W. van Kempen, *Physica* **C152**, 99 (1988).

[7] A.M. Okoniewski, J.E. Klemberg-Sapieha and A. Yelon, *Appl. Phys. Lett.* **53**, 151 (1988).

[8] R. Laiho, L. Heikkilä and H. Snellman, *J. Appl. Phys.* **63**, 225 (1988).

[9] M. Hangyo, S. Nakashima, K. Mizoguchi, A. Fujii and A. Mitsuishi, *Solid State Commun.* **65**, 835 (1988).

[10] S. Nakashima, M. Hangyo, K. Mizoguchi, A. Fujii, A. Mitsuishi and T. Yotsuga, *Jap. J. of Appl. Phys.* **26**, L1794 (1987).

[11] R.M. McFarlane, H. Rosen and H. Seki, *Solid State Commun.* **63**, 831 (1987).

[12] J. Giaever, *Phys. Rev. Lett.* **5**, 147 (1960); *Rev. Modern Phys.* **46**, 245 (1988).

[13] J. Giaever and H.P. Zeller, *Phys. Rev. Lett.* **20**, 1504 (1968).

[14] K. Mullen, E. Ben-Jacob, R.C. Jaklevic and Z. Schuss, *Phys. Rev. Lett.* **60**, 2543 (1988).

[15] R. Czajka, B. Susła, S. Szuba and J. Raułuszkiewicz, *Electron Technology* (Warsaw) **17**, 47 (1984).

[16] G. Binnig and D.P.E. Smith, *Rev. Sci. Instrum.* **57**, 8 (1986).

[17] A. Witek, L. Ornoch, A. Dąbkowski and J. Raułuszkiewicz, *Acta Physicae Superficierum* **II**, 51 (1990).

[18] C.S. Korman, J.C. Lau, A.M. Johnson and R.V. Coleman, *Phys. Rev.* **B19**, 994 (1979).

[19] K.W. Hipps, U. Mazur and M.S. Pearce, *Chem. Phys. Lett.* **68**, 433 (1979).